Mon. Not. R. Astron. Soc. **380,** 1581–1588 (2007) doi:10.1111/j.1365-2966.2007.12200.x

Experimental and theoretical transition probabilities in singly ionized gold

É. Biémont,[1,2]★ K. Blagoev,[3] V. Fivet,[2] G. Malcheva,[3] R. Mayo,[4,5] M. Ortiz[4] and P. Quinet[1,2]

[1]*IPNAS (Bât. B15), University of Liège, Sart Tilman, B-4000 Liège, Belgium*
[2]*Astrophysics and Spectroscopy, University of Mons-Hainaut, B-7000 Mons, Belgium*
[3] *Institute of Solid State Physics, Bulgarian Academy of Sciences, 72 Tzarigradsko Chaussee, BG-1784 Sofia, Bulgaria*
[4]*Faculty of Physics, Universidad Complutense de Madrid, E-28040 Madrid, Spain*
[5]*CIEMAT, Avda. Complutense 22, E-28040 Madrid, Spain*

Accepted 2007 July 2. Received 2007 July 2; in original form 2007 May 23

ABSTRACT

Absolute transition probabilities have been measured for lines originating from the $5d^9 6d$ and $5d^9 7s$ electronic configurations in the spectrum of singly ionized gold (Au II). The laser-induced breakdown spectroscopy has been applied to free gold atoms and ions produced by laser ablation. Absolute transition probabilities have been determined using the branching fraction and the Boltzmann plot methods. Theoretical branching fractions as well as radiative lifetime values have also been obtained by a relativistic Hartree–Fock method taking core polarization and configuration interaction effects into account. The new results are compared with previous results when available.

Key words: atomic data – atomic processes – line: identification.

1 INTRODUCTION

The investigation of stellar abundances of heavy elements, including gold, is important in astrophysics in relation with nucleosynthesis processes. In that field, new determination of accurate transition probabilities for singly ionized gold (Au II) lines is needed and timely, particularly for the analysis of chemically peculiar (CP) stars spectra.

Au II lines have indeed been identified in Ap and Bp stars (Fuhrmann 1989; Adelman 1994; Castelli & Hubrig 2004). The overabundances of some heavy elements, including gold, have also been extensively discussed in the literature (Wahlgren et al. 1995; Brandt et al. 1999; Wahlgren et al. 2001; Castelli & Hubrig 2004) and these investigations emphasize the need for additional determination of atomic parameters, particularly for singly ionized gold.

In plasma physics, gold is used as an active medium in metal vapour lasers. Numerous laser transitions, in the spectral range 253–763 nm, have been observed when exciting a helium discharge in a gold-plated hollow cathode by Reid et al. (1976). Consequently, the determination of accurate radiative parameters of Au II excited states, including transition probabilities, is of great interest.

Transition probabilities and oscillator strengths in the spectrum of singly ionized gold are rather sparse, particularly on the experimental side.

Transition probabilities of two-electron $5d^8(n+1)s^2$–$5d^9(n+1)p$ transitions in Au II spectrum have been evaluated in a Hartree–Fock approximation (length and velocity forms of the transition operator) by Blagoev et al. (1990). The radiative lifetimes of 11 excited states belonging to the $5d^9 6p$ electronic configuration of Au II have been measured by Beideck et al. (1993) with the beam–foil spectroscopy method. Theoretical lifetimes have been calculated by the same authors using the Cowan's codes (Cowan 1981). Radiative lifetimes of excited states belonging to the Au II $5d^9 6s$, $5d^9 6p$ and $5d^9 7s$ configurations and the transition probabilities of $5d^9 6s$–$5d^9 6p$, $5d^{10}$–$5d^9 6p$ and $5d^9 6p$–$5d^9 7s$ transitions have been obtained theoretically using a Hartree–Fock method in intermediate coupling by Loginov & Tuchkin (1998). In the paper of Rosberg & Wyart (1997), gf values for some transitions arising from the $5d^9 7p$, $5d^8 6s6p$, $5d^9 6p$, $5d^9 7s$, $5d^9 8s$, $5d^9 6d$ and $5d^7 6s^2 6p$ configurations of Au II have been calculated by Cowan's computer codes. Theoretical transition probabilities and oscillator strengths obtained with a method of superposition of configurations (length and velocity formalisms) have been published for $5d^{10}$–$5d^9 6p$ and $5d^9 6s$–$5d^9 6p$ transitions of Au II by Bogdanovich & Martinson (2000). In the same work, theoretical radiative lifetimes of the upper $5d^9 6p$ states of the investigated transitions have also been reported.

More recently, Zhang et al. (2002) reported the lifetimes for three of the $5d^9 6p$ excited levels of Au II measured with the time-resolved laser-induced fluorescence (TRLIF) method. The same lifetimes and the gf values for the $5d^9 6s$–$5d^9 6p$ transitions have been computed by a relativistic multiconfiguration Dirac–Fock (MCDF) method. Very recently, Fivet et al. (2006) measured the radiative lifetime of one $5d^9 6p$ level of Au II using the TRLIF technique as well, a lifetime which was found in agreement with the theoretical value obtained in the same paper by a relativistic Hartree–Fock (HFR) method taking core polarization and configuration interaction effects into account. In the same paper, oscillator strengths for sixty-three

★E-mail: E.Biemont@ulg.ac.be

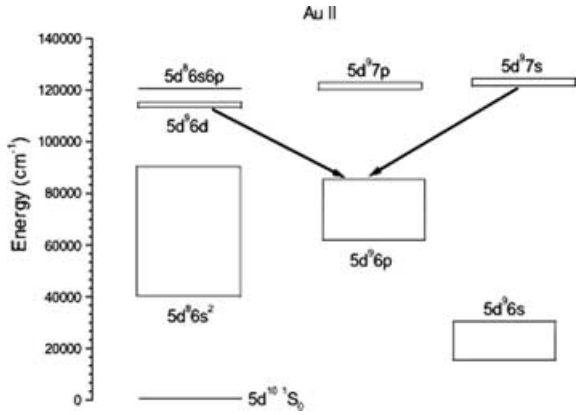

Figure 1. Schematic energy diagram of Au II. Only the few configurations of interest for this work are plotted on the figure.

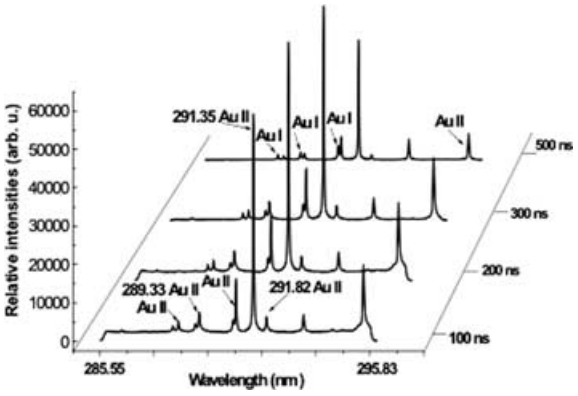

Figure 3. Time evolution of gold plasma. The relative intensities of some line are plotted as a function of the wavelength for different values of the delay (100–500 ns).

5d^{9}6s–5d^{9}6p, 5d^{9}6p–5d^{9}7s and 5d^{10}–5d^{9}6p ultraviolet transitions have been obtained.

In this paper, we report on transition probabilities for spectral lines of astrophysical interest emitted from 6d and 7s configurations of Au II (Fig. 1), transitions which, up to now, have not been considered experimentally. Some of the transitions included in the line list are of special interest for laser physics.

This work on Au II is the continuation of a long-term effort for improving the radiative data for heavy elements belonging to the sixth row of the periodic table. Some of the results obtained previously are stored in a data base created on a web site of Mons University (Fivet et al. 2007) (data base Database on Sixth Row Elements at the address: http://www.umh.ac.be/∼astro/desire.shtml) where the relevant references can be found.

2 EXPERIMENT

The measurements were carried out using the laser-induced breakdown spectroscopy (LIBS). A schematic diagram of the experimental setup is shown in Fig. 2. This experimental arrangement is similar to the one used in our previous works (Campos et al. 2005; Ortiz et al. 2007). Consequently, only a brief description is given here.

Free gold atoms and ions were produced by laser ablation using a Nd:YAG laser (YG 585 Quantel) at 1064 nm wavelength with

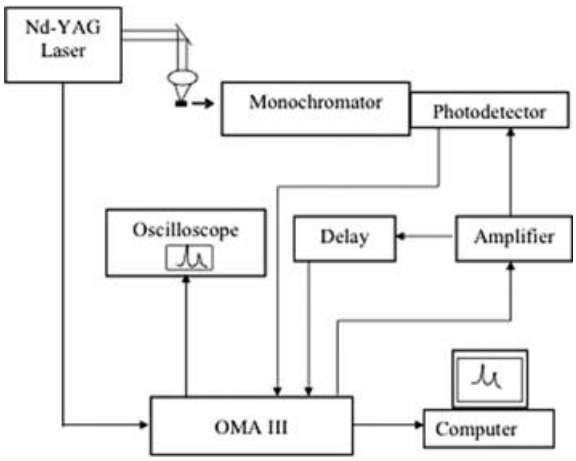

Figure 2. Experimental setup for branching fraction measurements (for a detailed description, see the text).

7 ns pulse duration at 20 Hz and 160 mJ pulse energy. The plasma is generated by focusing the laser beam on to the sample surface. The rotating target, made of 99.9999 per cent pure gold, was placed in a vacuum chamber filled with Ar at 8 Torr pressure. The light emission from the plasma was directed on to the entrance slit of a 1-m grating Czerny–Turner monochromator with 2400 groves/mm and 0.03 nm resolution. The gold spectrum was registered by a time-resolved optical multichannel analyzer system (OMA III, EG&G) having 1024 channels. This system allowed the recording of 10-nm spectrum sections. Every spectral region was registered after different delay times (i.e. 100, 200, 300 and 500 ns, respectively) following the laser pulse (Fig. 3). The examination of the plasma evolution with time provides the possibility of choosing the optimal value of this delay by retaining the best signal-to-noise ratio. We adopted the spectra registered at 200 ns after the laser pulse for the determination of the experimental transition probabilities. The experiment was carried out with a glass filter placed in front of the entrance slit of the monochromator allowing, in this way, to avoid the possible influence of the second order spectra.

The calibration of the spectral response of the experimental system and of the OMA photodiode array was determined according to the method described in our previous paper (Xu et al. 2004). The total error due to the calibration of the system is estimated at about 6 per cent.

In addition to Ar, the experiments were also carried out using Ne as buffer gas in order to detect Ar lines that could be responsible of blending problems with Au lines.

The spectral lines were analysed using a special software allowing to deduce the main line parameters, that is, the intensity, the width at half maximum, the Gaussian and the Lorentzian components of the profiles. With this programe, it was possible to calibrate the spectrum to substract the background and to separate the overlapping or closely spaced spectral lines. The intensities from 10 different measurements were averaged to determine the final value of each line.

The experimental relative transition probabilities were normalized using the theoretical estimates of the radiative lifetimes of the upper levels of the transitions as calculated in this work (see Section 3). The corresponding HFR lifetimes are reported in Table 1.

The transition probabilities for some of the transitions investigated in this work were determined using a Boltzmann plot. The hypothesis of local thermodynamic equilibrium (LTE) was made involving that the Saha and the Boltzmann laws were valid. For

Table 1. HFR lifetime values (in ns).

E (cm^{-1})[a]	Level[a]	τ (ns)[b]	E (cm^{-1})[a]	Level[a]	τ (ns)[b]
108 172.952	$7s(5/2,1/2)_3$	1.651	118 029.272	$6d(5/2,5/2)_2$	1.500
108 631.442	$7s(5/2,1/2)_2$	1.728	118 168.022	$6d(5/2,5/2)_4$	1.649
120 822.927	$7s(3/2,1/2)_1$	1.644	120 269.507	$6d(5/2,5/2)_0$	1.614
121 118.779	$7s(3/2,1/2)_2$	1.708	129 287.875	$6d(3/2,3/2)_1$	1.269
			129 560.535	$6d(3/2,3/2)_3$	0.981
116 050.55	$6d(5/2,3/2)_1$	1.012	129 918.201	$6d(3/2,5/2)_1$	1.176
116 946.327	$6d(5/2,3/2)_4$	1.011	130 198.661	$6d(3/2,5/2)_4$	1.575
117 065.629	$6d(5/2,3/2)_2$	1.080	130 266.093	$6d(3/2,3/2)_2$	1.277
117 297.679	$6d(5/2,5/2)_1$	1.513	130 464.446	$6d(3/2,5/2)_2$	1.277
117 346.060	$6d(5/2,5/2)_5$	1.529	130 749.252	$6d(3/2,5/2)_3$	1.612
117 511.998	$6d(5/2,3/2)_3$	1.084	131 563.734	$6d(3/2,3/2)_0$	1.491
117 983.169	$6d(5/2,5/2)_3$	1.526			

[a]From Rosberg & Wyart (1997)
[b]HFR values: this work.

satisfying the LTE hypothesis, the criterion proposed by Griem (1964) (see also Thorne 1988) was adopted:

$$N_e > 9.10^{17}\sqrt{\frac{kT}{13.6}}\left[\frac{\Delta E}{13.6}\right]^3, \quad (1)$$

where N_e is the electronic density in cm^{-3}, T is the temperature expressed in K and ΔE is the maximum energy difference in eV.

Considering that the ionic broadening parameter is negligible because its weight is generally lower than 2 per cent, it is possible to determine the electronic density by the formula:

$$N_e = 10^{16}\frac{\Delta\lambda}{\omega}, \quad (2)$$

where ω is the Stark broadening that can be found in the literature and $\Delta\lambda$ is the FWHM of the spectral line profile. Using the Boltzmann equation, the following formula can be written as

$$\ln\left(\frac{I}{gA}\right) = -\frac{E_{\rm upper}}{kT} + C, \quad (3)$$

where C is a constant.

For obtaining the plasma temperature, a Boltzmann plot has to be considered, that is, a plot of $\ln(I/gA)$ versus the energy of the upper level of the transition (Fig. 4). The plasma temperature can be obtained from the slope of this plot. Some of the transition probabilities of the spectral lines investigated in this work were determined using equation (3). They are marked with an asterisk in Column 6 of Tables 2 and 3. The plasma temperature was assumed to be $T = 18\,700 \pm 2000$ K and the adopted electron density was $N_e = (1.51 \pm 0.28) \times 10^{17}$ cm^{-3}. Since the limit for the Griem criterion is 3.4×10^{16} cm^{-3}, we can conclude that our plasma satisfies the LTE hypothesis.

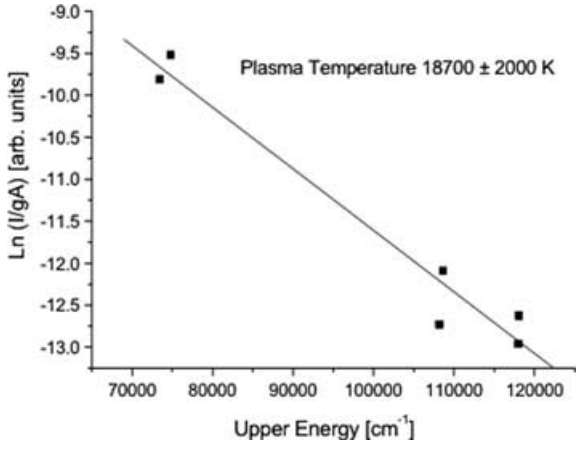

Figure 4. Boltzmann's plot for Au II. The estimated plasma temperature is $18\,700 \pm 2000$ K.

The value of the temperature was derived from a Boltzmann plot for Au II (Fig. 4) obtained with the line intensities of the present experiment and the transition probabilities calculated in this work. The lines used were $6s(3/2,1/2)_2$–$6p(5/2, 3/2)^\circ_{1,3}$, $6p(5/2, 3/2)^\circ_2$–$6d(5/2, 5/2)_3$, $6p(5/2, 3/2)^\circ_1$–$6d(5/2, 5/2)_2$, $6p(5/2, 1/2)^\circ_2$–$7s(5/2, 1/2)_3$ and $6p(5/2, 1/2)^\circ_3$–$7s(5/2, 1/2)_2$. By means of the Saha equation, we can infer that the plasma composition is N(Au II)/N(Au I) $\approx$ 309 and N(Au III)/N(Au II) $\approx$ 0.91.

The possible presence of self-absorption effects in the plasma was evaluated by considering the estimated electron density. Once the total density of Au II was deduced from the corresponding densities of the different species present in the plasma, the intensity of the absorption line could be integrated along the profiles for all the lines observed in the plasma. In fact, we calculated the ratio between the observed intensity and the one emitted by an optically thin plasma (the condition being that the optical depth is much lower than 1 (Thorne 1988)), that is,

$$K(\lambda)D \ll 1, \quad (4)$$

where $K(\lambda)$ is the self-absorption coefficient and D (expressed in cm) is the plasma thickness (estimated to be around 1 mm in our experiment). If this ratio exceeds 0.97, which would be equivalent to a self-absorption lower than 3 per cent, the plasma can be considered as optically thin. Since the largest effects were found to be lower than 3 per cent [for the Au II line at 192.457 nm with $K(\lambda) = 0.28$], we may consider that the self-absorption effects are negligible for the investigated transitions.

3 HFR CALCULATIONS

Gold is a heavy atom ($Z = 79$) and performing accurate atomic structure calculations in Au II requires that both relativistic and correlation effects are considered simultaneously. In the framework of the HFR approach (Cowan 1981), the relativistic corrections were the mass-velocity, the one-body Darwin terms and the Blume–Watson spin-orbit interaction. The latter contribution includes the part of the Breit interaction that can be reduced to a one-body operator. The correlation effects were included in different ways following the type of interactions, that is, valence–valence or core–valence contributions. Core–valence interactions were taken into account through a polarization model potential and a correction to the dipole operator according to a well-established procedure (see e.g. (Quinet et al. 1999)) giving rise to the HFR + Core-poralization (CPOL) method.

The calculations in Au II have been described previously (Fivet et al. 2006) and, consequently, only a short summary of these calculations is reported here.

The configurations retained explicitly in the model were: $5d^{10}$, $5d^96s$, $5d^97s$, $5d^98s$, $5d^96d$, $5d^97d$, $5d^86s^2$, $5d^87s^2$, $5d^86p^2$, $5d^87p^2$, $5d^86s7s$, $5d^86s6d$, $5d^76s^26d$ and $5d^76s6p^2$ (even parity), and $5d^96p$, $5d^97p$, $5d^95f$, $5d^96f$, $5d^86s6p$, $5d^86s7p$, $5d^86s5f$, $5d^86s6f$, $5d^76s^26p$, $5d^76s^25f$ and $5d^76s^26f$ (odd parity). The level values adopted for the fitting procedure were taken from Rosberg & Wyart (1997). These authors have thoroughly investigated the Au II spectrum and their analysis includes 450 classified lines and 120 energy levels. 37 even levels and 84 odd levels were retained in the fit of this work. The parameters (slater integrals) not adjusted in the calculation were

Table 2. Transition probabilities for $5d^9 6p$–$5d^9 7s$ lines of Au II. Only the transitions for which the values of $g_k A_{ki}$ are larger than 0.05×10^8 s^{-1} are quoted.

λ(nm)[a]	E(cm^{-1})[a]	Lower level design	E (cm^{-1})[a]	Upper level design	Exp.	$g_k A_{ki}(10^8$ s$^{-1})$ HFR	Previous
221.563 98	63 053.318	$6p(5/2,1/2)^\circ_2$	108 172.952	$7s(5/2,1/2)_3$	8.44 ± 0.54	15.07	15.24,[b] 15.26,[c] 15.26[d]
231.574 62	65 003.594	$6p(5/2,1/2)^\circ_3$			9.41 ± 0.97	7.55	7.67,[b] 7.84,[c] 8.05[d]
280.203 55	72 495.129	$6p(5/2,3/2)^\circ_4$			19.2 ± 1.7	14.18	14.76,[b] 14.42,[c] 14.42[d]
285.673 96	73 178.291	$6p(5/2,3/2)^\circ_2$			0.57 ± 0.11	0.30	0.43,[b] 0.42,[c] 0.35[d]
299.480 03	74 791.477	$6p(5/2,3/2)^\circ_3$			4.76 ± 0.76	5.21	5.03,[b] 5.53,[c] 5.46[d]
317.235 01	76 659.700	$6p(3/2,1/2)^\circ_2$			0.06 ± 0.01	0.02	0.02,[b] 0.02,[c] 0.03[d]
219.334 98	63 053.318	$6p(5/2,1/2)^\circ_2$	108 631.442	$7s(5/2,1/2)_2$	0.44 ± 0.06	0.85	0.94,[b] 0.85,[c] 0.85[d]
229.140 73	65 003.594	$6p(5/2,1/2)^\circ_3$			10.90 ± 0.96	13.30	13.30,[b] 12.30,[c] 12.10[d]
281.979 93	73 178.291	$6p(5/2,3/2)^\circ_2$			8.49 ± 0.68	6.96	6.66,[b] 7.25,[c] 7.20[d]
283.784 84	73 403.839	$6p(5/2,3/2)^\circ_1$			3.71 ± 0.92	3.34	3.45,[a] 3.65,[c] 3.15[d]
295.422 23	74 791.477	$6p(5/2,3/2)^\circ_3$			4.11 ± 0.65	3.38	3.66,[b] 3.60,[c] 3.90[d]
312.685 56	76 659.700	$6p(3/2,1/2)^\circ_2$			0.41 ± 0.05	0.23	0.20,[b] 0.15,[c] 0.25[d]
370.654 69	81 659.828	$6p(3/2,1/2)^\circ_1$			0.71 ± 0.10	0.63	0.70,[b] 0.35,[c] 0.40[d]
436.104 04	85 707.570	$6p(3/2,3/2)^\circ_1$			0.15 ±0.01	0.22	0.24,[b] 0.05,[c] 0.15[d]
209.820 58	73 178.291	$6p(5/2,3/2)^\circ_2$	120 822.927	$7s(3/2,1/2)_1$	0.28 ± 0.03	0.32	0.25,[b] 0.78,[c] 0.45[d]
226.362 68	76 659.700	$6p(3/2,1/2)^\circ_2$			7.90 ± 2.70	8.82	8.80,[b] 8.22,[c] 8.49[d]
255.265 80	81 659.828	$6p(3/2,1/2)^\circ_1$			1.08 ± 0.19	1.47	1.38,[b] 1.35,[c] 2.52[d]
261.639 32	82 613.781	$6p(3/2,3/2)^\circ_0$			2.26 ± 0.44	1.94	1.90,[b] 1.98,[c] 1.98[d]
284.692 02	85 707.570	$6p(3/2,3/2)^\circ_1$			3.71 ± 0.94	3.00	2.99,[b] 3.60,[c] 2.73[d]
291.823 47	86 565.667	$6p(3/2,3/2)^\circ_2$			3.07 ± 0.42	2.52	2.59,[b] 2.91,[c] 2.94[d]
208.525 61	73 178.291	$6p(5/2,3/2)^\circ_2$	121 118.779	$7s(3/2,1/2)_2$	-	0.38	0.18,[b] 0.02,[c] 0.40[d]
209.511 38	73 403.839	$6p(5/2,3/2)^\circ_1$			2.25 ± 0.29 *	2.93	3.25,[b] 2.55,[c] 3.65[d]
224.856 21	76 659.700	$6p(3/2,1/2)^\circ_2$			7.1 ± 2.2 *	5.93	6.03,[b] 6.45,[c] 6.10[d]
253.351 76	81 659.828	$6p(3/2,1/2)^\circ_1$			3.58 ± 0.42 *	4.21	3.77,[b] 3.95,[c] 2.75[d]
282.254 62[e]	85 700.201	$6p(3/2,3/2)^\circ_3$			13.0 ± 2.0 *	10.53	10.54,[b] 10.65,[c] 11.00[d]
282.313 35	85 707.570	$6p(3/2,3/2)^\circ_1$			-	1.15	1.45,[b] 0.80,[c] 1.25[d]
289.324 68	86 565.667	$6p(3/2,3/2)^\circ_2$			4.32 ± 0.81 *	3.80	3.64,[b] 4.15,[c] 4.20[d]

*Obtained from Boltzmann's plot.
[a]From Rosberg & Wyart (1997).
The underlined wavelengths are of special interest for laser physics (see the text).
[b]From Rosberg & Wyart (1997).
[c]From Loginov & Tuchkin (1998): the parameters used in the calculations were obtained from a Newton's method.
[d]From Loginov & Tuchkin (1998): the parameters used in the calculations were obtained by a least-squares fit.
Exp.: this work.
HFR: this work.
[e]Blended with λ 282.313 35.

scaled down by 0.85 while the spin-orbit integrals were kept at their *ab initio* values. The mean deviations obtained reached 66 cm^{-1} (even parity) and 194 cm^{-1} (odd parity), respectively. The value of the dipole polarizability was adopted from Fraga, Karwowski & Saxena (1976), that is, $\alpha_d = 4.45$ au, while the cut-off radius, which corresponds to the mean value $< r >$ of the outermost orbital of the core $5d^7$, was chosen equal to $r_c = 1.47$ au.

The Au II HFR lifetime values reported by Fivet et al. (2006) for the $5d^9 6p$ configuration were found to agree well with experiment (Beideck et al. 1993; Zhang et al. 2002), the only exception being the level at 85 708 cm^{-1}. For 76 660 cm^{-1}, the HFR value, in good agreement with the MCDF value, confirmed the laser-induced fluorescence measurements of Zhang et al. (2002) but not the beam–foil measurement of Beideck et al. (1993). The lifetimes calculated by Bogdanovich & Martinson (2000) and, to a lesser extent, by Beideck et al. (1993) (HFR approach), were found systematically to be too low (lower than all the other results), the discrepancies being attributed to the rather simple model adopted by these authors that did not take the CPOL effects into account.

The oscillator strengths of the $5d^9 6p$–$5d^9 6d$ and $5d^9 6p$–$5d^9 7s$ transitions of Au II are reported in Tables 2 and 3. In our previous paper, the HFR oscillator strengths for the $5d^9 6s$–$5d^9 6p$ transitions did agree quite well with the MCDF results. Large discrepancies with the results of Rosberg & Wyart (1997), also obtained with Cowan's code, were observed and could be explained by the fact that Rosberg & Wyart (1997) have considered, in their calculations, a very limited number of configurations (in fact the configurations observed experimentally) and have not retained the CPOL effects.

Table 3. Transition probabilities for $5d^9 6p$–$5d^9 6d$ lines of Au II. Only the transitions for which the values of $g_k A_{ki}$ are larger than 0.05×10^8 s^{-1} are quoted.

λ(nm)	E (cm^{-1})[b]	Lower level design	E (cm^{-1})[b]	Upper level design	$g_k A_{ki}$ (10^8 s^{-1}) Exp.	HFR	Previous[c]
188.689 10[b]	63 053.318	$6p(5/2,1/2)^\circ_2$	116 050.55	$6d(5/2,3/2)_1$	–	27.42	31.10
233.180	73 178.291	$6p(5/2,3/2)^\circ_2$			1.58 ± 0.21[a]	1.41	
234.414	73 403.839	$6p(5/2,3/2)^\circ_1$			–	0.57	
253.791	76 659.700	$6p(3/2,1/2)^\circ_2$			–	0.10	
290.692	81 659.828	$6p(3/2,1/2)^\circ_1$			–	0.07	
192.519 72[b]	65 003.594	$6p(5/2,1/2)^\circ_3$	116 946.327	$6d(5/2,3/2)_4$	56 ± 13[a]	80.98	96.66
224.896 06[b]	72 495.129	$6p(5/2,3/2)^\circ_4$			4.2 ± 1.8[a]	3.86	5.25
237.148 22[b]	74 791.477	$6p(5/2,3/2)^\circ_3$			4.3 ± 1.1[a]	4.11	4.51
185.081	63 053.318	$6p(5/2,1/2)^\circ_2$	117 065.629	$6d(5/2,3/2)_2$	–	32.32	42.58
192.016	65 003.594	$6p(5/2,1/2)^\circ_3$			6.4 ± 1.7[a]	6.36	
227.787	73 178.291	$6p(5/2,3/2)^\circ_2$			–	1.06	
236.478 89[b]	74 791.477	$6p(5/2,3/2)^\circ_3$			9.9 ± 2.7[a]	6.42	6.55
327.776	86 565.667	$6p(3/2,3/2)^\circ_2$			0.10 ± 0.02[a]	0.01	
184.289	63 053.318	$6p(5/2,1/2)^\circ_2$	117 297.679	$6d(5/2,5/2)_1$	–	3.38	5.53
226.587 63[b]	73 178.291	$6p(5/2,3/2)^\circ_2$			3.07 ± 0.92[a]	3.61	4.01
227.752 06[b,d]	73 403.839	$6p(5/2,3/2)^\circ_1$			12.5 ± 2.9[a]	9.34	10.69
280.517 84[b]	81 659.828	$6p(3/2,1/2)^\circ_1$			2.27 ± 0.30[a]	2.72	3.08
316.463 21[b]	85 707.570	$6p(3/2,3/2)^\circ_1$			0.46 ± 0.08[a]	0.71	0.78
222.891 51[b,e]	72 495.129	$6p(5/2,3/2)^\circ_4$	117 346.06	$6d(5/2,5/2)_5$	62.9 ± 7.1[a]	71.80	84.71
183.564	63 053.318	$6p(5/2,1/2)^\circ_2$	117 511.998	$6d(5/2,3/2)_3$	–	23.27	27.95
190.383	65 003.594	$6p(5/2,1/2)^\circ_3$				27.31	35.05
222.069 85[b]	72 495.129	$6p(5/2,3/2)^\circ_4$			–	3.29	3.72
225.492 13[b]	73 178.291	$6p(5/2,3/2)^\circ_2$			1.99 ± 0.39[a]	1.34	1.28
234.007 82[b]	74 791.477	$6p(5/2,3/2)^\circ_3$			9.6 ± 2.2[a]	9.09	10.60
181.989	63 053.318	$6p(5/2,1/2)^\circ_2$	117 983.169	$6d(5/2,5/2)_3$	–	0.08	
188.690	65 003.594	$6p(5/2,1/2)^\circ_3$			–	5.00	5.53
219.769 43[b]	72 495.129	$6p(5/2,3/2)^\circ_4$			–	0.45	0.42
223.120 62[b]	73 178.291	$6p(5/2,3/2)^\circ_2$			25.4 ± 5.2[a]	27.25	32.87
231.454 85[b]	74 791.477	$6p(5/2,3/2)^\circ_3$			17.5 ± 4.5[a]	11.94	15.31
241.919 66[b]	76 659.700	$6p(3/2,1/2)^\circ_2$			–	0.99	1.09
181.897 65[b]	63 053.318	$6p(5/2,1/2)^\circ_2$	118 029.272	$6d(5/2,5/2)_2$	–	2.96	1.03
188.587 86[b]	65 003.594	$6p(5/2,1/2)^\circ_3$			–	2.28	1.30
222.891 51[b,e]	73 178.291	$6p(5/2,3/2)^\circ_2$			45.9 ± 6.9[a]	17.35	22.91
224.017 91[b]	73 403.839	$6p(5/2,3/2)^\circ_1$			8.0 ± 2.0[a]	7.41	8.38
231.208 02[b]	74 791.477	$6p(5/2,3/2)^\circ_3$			–	0.59	1.50
241.650 15[b]	76 659.700	$6p(3/2,1/2)^\circ_2$			0.61 ± 0.08[a]	0.87	0.85
274.874 78[b]	81 659.828	$6p(3/2,1/2)^\circ_1$			–	1.34	2.07
309.299 87[b]	85 707.570	$6p(3/2,3/2)^\circ_1$			0.52 ± 0.08[a]	0.48	0.68
188.095 69[b]	65 003.594	$6p(5/2,1/2)^\circ_3$	118 168.022	$6d(5/2,5/2)_4$	–	1.18	0.90
218.879 77[b]	72 495.129	$6p(5/2,3/2)^\circ_4$				16.87	21.06
230.468 42[b]	74 791.477	$6p(5/2,3/2)^\circ_3$				36.23	44.54
213.308 52[b]	73 403.839	$6p(5/2,3/2)^\circ_1$	120 269.507	$6d(5/2,5/2)_0$	3.07 ± 0.45[a]	5.91	7.18
258.925 00[b]	81 659.828	$6p(3/2,1/2)^\circ_1$			0.45 ± 0.09[a]	0.13	0.39
289.250 79[b]	85 707.570	$6p(3/2,3/2)^\circ_1$			–	0.13	0.19
178.162	73 178.291	$6p(5/2,3/2)^\circ_2$	129 287.875	$6d(3/2,3/2)_1$	–	0.16	
178.881	73 403.839	$6p(5/2,3/2)^\circ_1$			–	5.31	7.56
189.950	76 659.700	$6p(3/2,1/2)^\circ_2$			1.67 ± 0.55[a]	1.11	

Table 3 – *continued*

λ(nm)	E (cm^{-1})[b]	Lower level design	E (cm^{-1})[b]	Upper level design	Exp.	g_kA_{ki}(10^8 s^{-1}) HFR	Previous[c]
209.894	81 659.828	$6p(3/2,1/2)^\circ_1$			3.27 ± 0.48[a]	3.54	
214.231[f]	82 613.781	$6p(3/2,3/2)^\circ_0$			1.30 ± 0.17[a]	3.50	
229.390 75[b]	85 707.570	$6p(3/2,3/2)^\circ_1$			7.4 ± 1.2[a]	7.28	7.63
233.999	86 565.667	$6p(3/2,3/2)^\circ_2$			–	2.54	
177.300	73 178.291	$6p(5/2,3/2)^\circ_2$	129 560.535	$6d(3/2,3/2)_3$	–	3.27	
189.033 00[b]	76 659.700	$6p(3/2,1/2)^\circ_2$			–	62.11	72.63
227.927	85 700.201	$6p(3/2,3/2)^\circ_3$			4.2 ± 1.1[a]	3.34	
232.514 51[b,g]	86 565.667	$6p(3/2,3/2)^\circ_2$			1.77 ± 0.28[a]	2.39	2.70
176.182	73 178.291	$6p(5/2,3/2)^\circ_2$	129 918.201	$6d(3/2,5/2)_1$	–	0.18	
176.885	73 403.839	$6p(5/2,3/2)^\circ_1$			–	2.34	
187.701	76 659.700	$6p(3/2,1/2)^\circ_2$			–	2.26	
207.151 83[b]	81 659.828	$6p(3/2,1/2)^\circ_1$				11.21	9.80
211.329 84[b,h]	82 613.781	$6p(3/2,3/2)^\circ_0$			13.2 ± 2.1[a]	8.06	11.32
226.119 89[b]	85 707.570	$6p(3/2,3/2)^\circ_1$			0.89 ± 0.23[a]	0.98	2.48
230.597	86 565.667	$6p(3/2,3/2)^\circ_2$			–	0.25	
153.327	65 003.594	$6p(5/2,1/2)^\circ_3$	130 198.661	$6d(3/2,5/2)_4$	–	0.26	0.12
224.657 20[b]	85 700.201	$6p(3/2,3/2)^\circ_3$			47.5 ± 9.7[a]	56.15	2.64
148.722	63 053.318	$6p(5/2,1/2)^\circ_2$	130 266.09	$6d(3/2,3/2)_2$	–	0.1	
175.108	73 178.291	$6p(5/2,3/2)^\circ_2$			–	0.44	
175.863 54[b]	73 403.839	$6p(5/2,3/2)^\circ_1$			–	6.21	7.14
186.544 90[b]	76 659.700	$6p(3/2,1/2)^\circ_2$			–	8.55	17.09
205.668 64[b]	81 659.828	$6p(3/2,1/2)^\circ_1$			3.5 ± 1.3[a]	4.4	9.94
224.318	85 700.201	$6p(3/2,3/2)^\circ_3$			–	1.9	
224.355	85 707.570	$6p(3/2,3/2)^\circ_1$			5.2 ± 1.6[a]	4.67	
228.760 18[b]	86 565.667	$6p(3/2,3/2)^\circ_2$				12.14	11.35
174.502	73 178.291	$6p(5/2,3/2)^\circ_2$	130 464.446	$6d(3/2,5/2)_2$	–	0.67	
175.192	73 403.839	$6p(5/2,3/2)^\circ_1$			–	0.19	
185.857 27[b]	766 59.700	$6p(3/2,1/2)^\circ_2$				10.85	7.18
204.832 96[b]	81 659.828	$6p(3/2,1/2)^\circ_1$				12.84	10.74
223.324	85 700.201	$6p(3/2,3/2)^\circ_3$			–	0.07	
223.359 96[b,i]	85 707.570	$6p(3/2,3/2)^\circ_1$			18.6 ± 6.3[a]	12.85	18.03
227.726 43[b]	86 565.667	$6p(3/2,3/2)^\circ_2$			–	1.03	4.46
147.661	63 053.318	$6p(5/2,1/2)^\circ_2$	130 749.252	$6d(3/2,5/2)_3$	–	0.39	0.17
173.698 69[b]	73 178.291	$6p(5/2,3/2)^\circ_2$			–	0.19	0.16
184.878 46[b]	76 659.700	$6p(3/2,1/2)^\circ_2$				0.50	0.60
221.911 18[b]	85 700.201	$6p(3/2,3/2)^\circ_3$			8.2 ± 1.1	10.72	12.93
226.258 37[b]	86 565.667	$6p(3/2,3/2)^\circ_2$			35.3 ± 8.4	29.9	35.87
171.880	73 403.839	$6p(5/2,3/2)^\circ_1$	131 563.734	$6d(3/2,3/2)_0$	–	2.77	2.06
200.320 25[b]	81 659.828	$6p(3/2,1/2)^\circ_1$			1.65 ± 0.27[a]	2.97	6.32
218.004 91[b]	85 707.570	$6p(3/2,3/2)^\circ_1$			1.32 ± 0.43[a]	0.85	2.28

Exp.: this work.
HFR: this work.
[a]Evaluated from Boltzmann's plot.
[b]From Rosberg & Wyart (1997); otherwise from NIST atomic data base.
[c]From Rosberg & Wyart (1997).
[d]The transition at 227.752 06 is blended with the 6p–6d transition at λ 227.787.
[e]Blend of λ 222.89 151 [$6p(5/2,3/2)^\circ_4$–$6d(5/2,5/2)_5$] with 222.89 151 [$6p(5/2,3/2)^\circ_2$–$6d(5/2,5/2)_2$].
[f]Blend with the $6s^2$–6s6p transition at 214.29 467 nm.
[g]Blend with the $6s^2$–6s6p transition at 232.57 108 nm.
[h]Blend with the $6s^2$–6s6p transition at 211.35 955 nm.
[i]Blend with λ 223.324.

Our calculations, which do include more correlation effects, are in good agreement with the MCDF data of Zhang et al. (2002). Similar considerations apply to the $5d^{10}$–$5d^{9}6p$ transitions. A better agreement with the calculations of Rosberg & Wyart (1997) is observed for the $5d^{9}6p$–$5d^{9}7s$ transitions but it should be emphasized that, for these transitions, CPOL effects are much smaller.

4 RESULTS AND DISCUSSION

The experimental and the theoretical transition probability values obtained in this work are presented in Tables 2 and 3 for 6p–7s and 6p–6d transitions, respectively, where they are compared with previous results when available (Rosberg & Wyart 1997; Loginov & Tuchkin 1998). The wavelengths and energy levels are taken from Rosberg & Wyart (1997). The wavelengths taken from older compilations (Harrison 1939; Zaidel et al. 1968) were also considered. Some wavelengths, not observed in Rosberg & Wyart (1997), whose upper levels belong to the 6d states with energies larger than 129 287 cm^{-1}, were calculated using the energy levels taken from Rosberg & Wyart (1997) and from Moore's tables (Moore 1958).

The experimental relative transition probabilities were converted into an absolute scale using the HFR theoretical values for the radiative lifetimes calculated in this work and reported in Table 1.

The gA values evaluated from a Boltzmann's plot are indicated with an asterisk (Table 2) or with the letter a (Table 3). The spectral lines of special interest for laser physics (Ivanov, Latush & Sem 1996) are underlined. These laser lines have been observed in quasi-CW and CW hollow cathode discharges using He as a buffer gas (Reid et al. 1976; Jain 1980).

In the evaluation of the total errors, the contributions arising from the calibration of the recording system as well as those originating from the statistical errors and from the plasma temperature determination were taken into account. The total experimental errors are, for almost all the transitions, included in between 6 and 25 per cent for the measured transition probabilities and in between 14 and 32 per cent for the values obtained from a Boltzmann's plot.

For some transitions, there are no experimental transition probabilities reported in the tables. This is due either to the fact that the corresponding wavelengths were outside of the accessible spectral range (190–600 nm) or to blending problems of the lines with other gold transitions or with transitions originating from the buffer gas.

For most of the lines, we observe a good agreement between the experimental transition probabilities and the HFR ones keeping in mind that the results derived from the Boltzmann's plots are affected by larger uncertainties.

Some of the theory–experiment discrepancies can be explained by blending problems affecting the measurements which are due to $6s^2$–6s6p and 6p–6d Au II transitions. The details can be found in the notes to Tables 2 and 3. Some differences remain unexplained for a few lines, the most notable case being the 6s–6p transition at 221.56 398 nm for which a discrepancy reaching a factor of 2 is observed between the experiment and the different theoretical values (which are in good agreement).

The agreement of our HFR values with previously published results (Rosberg & Wyart 1997; Loginov & Tuchkin 1998) is also reasonable, the discrepancies observed with the results of Rosberg & Wyart (1997) being explained by the fact that these authors did consider configuration interaction effects in a more limited way and, more particularly, did not take core polarization effects into account.

5 CONCLUSIONS

The absolute transition probabilities of the transitions originating from the $5d^{9}6d$ and $5d^{9}7s$ electronic configurations of Au II have been measured from a combination of lifetime calculations by the HFR method and of relative measurements by the LIBS method. These first experimental results for the 6p–6d and 6p–7s transitions agree reasonably well with the theoretical results obtained with a relativistic Hartree–Fock method, taking core polarization effects into account. There is also generally a good agreement with previously published results.

In the few cases where a discrepancy is observed between the theoretical and the experimental scales of A values, we would suggest to adopt as a first choice the experimental results which are considered as the best results presently available for these transitions.

This first set of experimental results is expected to be useful not only for the astrophysicists but also for the physicists working in plasma physics and in laser physics.

ACKNOWLEDGMENTS

The present work was financially supported by National Science Fund of Bulgaria (grant 1516/05) and Spanish DGICYT (project FIS2006-10117). Financial support from the Belgian FNRS is also acknowledged. EB and PQ are Research Director and Research Associate of this organism, respectively. VF has a FRIA fellowship.

REFERENCES

Adelman S. J., 1994, MNRAS, 266, 97
Beideck D. J., Curtis L. J., Irving R. E., Maniak S. T., Hellborg R., Johansson S. G., Martinson I., Rosberg M., 1993, J. Opt. Soc. Am. B, 10, 977
Blagoev K., Dimitrov N., Benhalla A., Bogdanovich P., Momkauskaite A., Rudzikas Z. B., 1990, Phys. Scr., 41, 213
Bogdanovich P., Martinson I., 2000, Phys. Scr., 61, 142
Brandt J. C. et al., 1999, AJ, 117, 1505
Campos J., Ortiz M., Mayo R., Biémont É., Quinet P., Blagoev K., Malcheva G., 2005, MNRAS, 363, 905
Castelli F. H. S., 2004, A&A, 425, 263
Cowan R. D., 1981, The Theory of Atomic Structure and Spectra, Univ. of California Press, Berkeley, USA
Fivet V., Quinet P., Biémont É., Xu H. L., 2006, J. Phys. B, 39, 3587
Fivet V., Quinet P., Palmeri P., Biémont É., Xu H. L., 2007, J. Electron Spectrosc. Relat. Phenom., 156, 250
Fraga S., Karwowski J., Saxena K. M. S., 1976, Handbook of Atomic Data, Elsevier, Amsterdam
Fuhrmann K., 1989, A&AS, 77, 345
Griem H. R., 1964, Plasma Spectroscopy, McGraw-Hill, New York
Harrison G. R., 1939, MIT Wavelength Tables. Wiley, New York
Ivanov I. G., Latush E. L., Sem M. F., 1996, Metal Vapour Ion Lasers, John Wiley & Sons, England
Jain K., 1980, J. Quantum Electron., QE-16, 387
Loginov A. V., Tuchkin V. I., 1998, Opt. Spectrosc., 85, 1
Moore C. E., 1958, Atomic Energy Levels, Vol. III, Nat. Bur. Stand. Circ. 467. US Government Printing Office, Washington DC, USA
Ortiz M., Mayo R., Biémont É. Q. P., Malcheva G., Blagoev K., 2007, J. Phys. B, 40, 167
Quinet P., Palmeri P., Biémont É, McCurdy M. M., Rieger G., Pinnington E. H., Lawler J. E., Wickliffe M. E., 1999, MNRAS, 307, 934
Reid R. D., McNeil J. R., Collins G. J., 1976, Appl. Phys. Lett., 29(10), 666

Rosberg M., Wyart J.-F., 1997, Phys. Scr., 55, 690
Thorne A., 1988, Spectrophysics. Chapman and Hall Ltd, London
Wahlgren G. M., Leckrone D. S., Johansson S. G., Rosberg M., Brage T., 1995, AJ, 444, 438
Wahlgren G. M. et al., 2001, ApJ, 551, 520
Xu H. L. et al., 2004, Phys. Rev. A, 70, 042508
Zaidel A. N., Prokofiev V. K., Raiskii S. M., Slavnii V. A., Schreider E. Ya, 1968, Tables of Spectral Lines. IFI/Plenum, New York
Zhang Z., Brage T., Curtis L. J., Lundberg H., Martinson I., 2002, J. Phys. B, 35, 483

This paper has been typeset from a TEX/LATEX file prepared by the author.